$\mathcal{H}_2$-optimal Control of an Adaptive Optics System: Part II, Closed-loop controller design

Karel Hinnen[a], Niek Doelman[b], Michel Verhaegen[a]

[a]Delft Center for Systems and Control, Mekelweg 2, 2628 Delft, The Netherlands;
[b]TNO Science and Industry, PO Box 155, 2600 AD Delft, The Netherlands

ABSTRACT

The problem of finding the closed-loop optimal controller is formulated in an $\mathcal{H}_2$-optimal control framework. This provides a natural way to account for the fact that in many AO systems the wavefront phase cannot be measured directly. Given a multi-variable disturbance model of both wavefront slopes and wavefront phases,[3] this provides a general procedure to compute the closed-loop controller. If the wavefront sensor and deformable mirror are static and the only dynamics in the system is a unit-sample delay between measurement and correction, an analytical expression for the optimal controller can be derived. This results in a control approach, in which both identification and computation of the optimal controller are exclusively based on standard matrix operations. No Riccati equation needs to be solved to compute the optimal controller. The proposed $\mathcal{H}_2$-control approach is numerically validated on open-loop wavefront sensor data and its performance is compared with the common approach. Also the sensitivity to measurement noise is considered.

Keywords: Adaptive optics, optimal control, spatial-temporal correlation, data-driven disturbance modeling

1. INTRODUCTION

The control strategy used in the current generation of AO system is generally not able to take full advantage of the spatio-temporal correlation in the wavefront disturbance. In the common AO control approach[1,2] the temporal correlation in the wavefront distortion is often neglected. Furthermore, the common control law is based on the open-loop hypothesis which assumes that the spatial wavefront statistics do not change under closed-loop operation. It is to be expected that a lot can be gained by using a rigorous control strategy that is able to account for both the dynamics of the wavefront, the AO system components and the modified statistics due to closed loop behavior. The performance of an AO control system is usually limited by the presence of measurement noise and the time delay between measurement and correction. By including the temporal aspect it is possible to anticipate on future distortions and reduce the effect of the time delay. Also the sensitivity to measurement noise may be reduced by including the spatio-temporal correlation. Photons from different time instants and different wavefront sensor (WFS) channels may all contribute to improve the wavefront estimate at a certain position in the aperture plane. This may possibly contribute to a reduction of the residual phase error or an increase of the required magnitude of the guide star.

In this paper we present a control strategy that is able to take full advantage of the spatio-temporal correlation of the wavefront. The AO control problem is analyzed from a control perspective where each WFS sensor channel is conceived as a separate input to the controller. The AO control problem is interpreted as a multi-variable discrete-time disturbance rejection problem. With the objective of minimizing the mean square residual wavefront error, the problem will be formulated in a $\mathcal{H}_2$-optimal control framework. In contrast to the common approach wavefront reconstruction is not seen as an isolated problem, but it forms as an integral part of the problem. The $\mathcal{H}_2$-optimal control framework provides an attractive way to deal with the discrepancy between the the closed-loop WFS signal that is measured and the residual wavefront that is minimized. In fact, part of the wavefront reconstruction has already been performed in the identification of the disturbance model, which forms the starting point in the computation of the closed-loop controller. The procedure used to identify a spatio-temporal disturbance model from open-loop WFS measurements is described in the companion paper.[3]

Further author information: (Send correspondence to K. Hinnen)
e-mail: k.j.g.hinnen@dcsc.tudelft.nl, Telephone: +31 (0)15 2786707

Astronomical Adaptive Optics Systems and Applications II, edited by Robert K. Tyson, Michael Lloyd-Hart,
Proceedings of SPIE Vol. 5903, 59030A, (2005) · 0277-786X/05/$15 · doi: 10.1117/12.614410

The remainder of this paper is organized as follows. Section 2 provides an accurate description of the considered AO control problem and introduces a projection to deal with the fact that part of the wavefront cannot be reconstructed from the WFS measurements. Section 3 first describes a general strategy to determine the optimal controller that minimizes the mean square residual phase error. The strategy consists of formulating the AO problem as a $\mathcal{H}_2$-optimal control problem for which there exists a standard solution. Subsequently, we elaborate the specific case of a quasi-static AO system where the WFS and DM are assumed to be static and only dynamics in the system is a unit-sample delay between measurement and correction. This results in an analytical expression for the closed-loop optimal controller. Section presents a numerical validation study, in which the performance of the proposed control approach is compared with the common AO control law. Also the effect of measuring noise will be analyzed in detail. The paper concludes with a short discussion in Section 5.

2. PROBLEM FORMULATION

To explain the central control problem in this paper, consider the block-scheme in Figure 1. It provides a schematic representation of the functional relation between the main components of a classical AO system. Light with an atmospherically distorted phase profile $\phi(\cdot)$ enters the system and is reflected from a deformable mirror (DM), which is able to introduce a phase correction ϕ^{dm}. Part of the compensated light, with residual phase error $\epsilon = \phi - \phi^{dm}$, is directed to a wavefront sensor (WFS). The WFS signal $s(\cdot)$ forms the input to the controller $\tilde{C}(z)$, which is responsible for determining the actuator commands $u(\cdot)$. The effect of measurement noise is represented by an additive noise term η at the output of the WFS. A common objective of such an AO system is to maximize the Strehl ratio, which is defined as the on-axis intensity of a point source relative to that of the diffraction limit. Through the Marechal[4] approximation, this is equivalent to minimizing the mean square residual phase error. The AO control problem can hence be defined as the problem of finding the closed-loop controller $\tilde{C}(z)$ that minimizes the mean square residual phase error for the prevalent turbulence conditions.

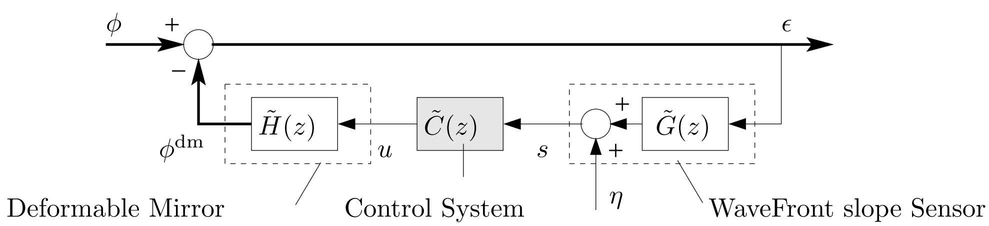

Figure 1. Schematic representation of the adaptive optics control problem

The above problem formulation is still too general and needs to be refined in order to arrive at a well-posed control problem. In this paper we will assume that the phase distortion profile over the aperture can represented by a finite-dimensional vector signal. This implies that at each time instant k, the uncorrected wavefront distortion $\phi(\cdot)$, the phase profile introduced by the DM $\phi_k^{dm}(\cdot)$ and the residual wavefront error $\epsilon(\cdot)$ can be specified by the finite-dimensional vectors $\phi_k \in \mathbb{R}^{m_p}$, $\phi_k^{dm} \in \mathbb{R}^{m_p}$ and $\epsilon_k \in \mathbb{R}^{m_p}$. Whether the vector signal ϕ_k provides a zonal or model description of the wavefront is irrelevant as long as the squared 2-norm $\|\phi\|_2^2 = \phi_k^T \phi_k$ provides an accurate estimate of the mean square phase over the aperture and the basis or sampling grid for describing the residual phase distortion and the phase introduced by the mirror is the same. Furthermore it is assumed that WFS can be described as the cascade of a static matrix multiplication that describes the optical transformation from phase ϵ_k to wavefront slope measurements s_k, a linear time invariant (LTI) system that accounts for any dynamics of the WFS camera and acquisition hardware and an additive white noise η_k term that models the measurement noise, i.e.

$$s_k = \tilde{G}(z)\epsilon_k + \eta_k, \tag{1}$$

where $\tilde{G}(z) = G\bar{G}(z)$ and z represents the z-transform parameter. An important complication in the AO control problem is that the WFS is not able to directly measure the residual phase $\epsilon_k \in \mathbb{R}^{m_p}$. Instead of measuring the phase, it usually provides a measure of the local slope of the wavefront from which it is not possible to reconstruct the entire wavefront. As the controller is not able to actively influence the unobservable part of the wavefront, the unobservable modes have to be excluded in order to arrive at a well-posed control problem. From equation (1) it is clear that only the part of the wavefront that is in the column space of G can be observed. With U_1 and V_1^T the left and right non-singular vectors of G, it is therefore useful to introduce the alternative signals $y_k \triangleq U_1^T s_k \in \mathbb{R}^{m_r}$ and $\varepsilon_k \triangleq V_1^T \bar{G}(z)\epsilon_k \in \mathbb{R}^{m_r}$ (see also[3]). By pre-multiplying equation (1), this leads to the reduced WFS model

$$y_k = \Sigma_1 \varepsilon_k + U_1^T \eta_k, \tag{2}$$

where Σ_1 is composed of the non-zero values of G and y_k takes over the task of the WFS measurement signal. When the wavefront dynamics can be neglected, i.e. $\tilde{G}(z) = G$, the signal ε_k can be interpreted as a reduced representation of observable part of the wavefront. In all other cases, ε_k will be colored by the WFS dynamics. Even when the WFS dynamics are explicitly known it is usually not sensible to compensate for it as it will increase the sensitivity to measurement noise. Also the DM is assumed to be described by an LTI system. The transfer function $H(z) = V_1^T \tilde{H}(z)$ should provide a mapping from actuator inputs u_k to the reduced DM phase profile, which in accordance with the observable part of the residual wavefront ε_k is defined as $\psi_k^{dm} \triangleq V_1^T \bar{G}(z)\phi_k^{dm}$. Likewise, the reduced counter parts of the uncorrected wavefront ϕ_k and the corresponding open-loop WFS signal are defined as $\psi_k \triangleq V_1^T \bar{G}(z)\phi_k$ and $r_k \triangleq \Sigma_1 \psi_k + U_1^T \eta_k$. The reduced representation of the observable part of the residual wavefront is defined as $\varepsilon_k \triangleq \psi_k - \psi_k^{dm}$.

Optimizing the AO system performance to the prevalent turbulence conditions requires an accurate description of the statistical properties of the uncorrected wavefront and the corresponding WFS signal. In this paper we assume that the observable part of the uncorrected wavefront ψ_k and the measured reduced WFS signal r_k can be modeled as the output of a stable LTI filter with a zero-mean white noise input $v_k \in \mathbb{R}^{m_r}$. More specifically, we will assume that the atmospheric disturbance is described by the following state space model:

$$S: \left\{ \begin{array}{rcrcr} x_{k+1} &=& A\,x_k &+& Kv_k \\ r_k &=& \Sigma_1 C\,x_k &+& v_k \\ \psi_k &=& C\,x_k &+& e_k \end{array} \right. , \qquad \mathcal{E}\left(\begin{bmatrix} v_k \\ e_k \\ I \end{bmatrix} \begin{bmatrix} v_l^T & e_l^T \end{bmatrix} \right) = \begin{bmatrix} R_v & R_{ev}^T \\ R_{ev} & R_e \\ 0 & 0 \end{bmatrix} \delta_{kl}. \tag{3}$$

where e_k is another zero-mean white noise signal which is likely to be correlated with v_k. The description of the open-loop WFS r_k provided by the atmospheric disturbance model S includes the contribution due to measurement noise $U_1^T \eta$. The motivation for this particular model structure and the problem of how to identify such disturbance model form open loop WFS data are considered in a companion paper.[3] For a given disturbance model $S(z)$, the control problem can now be formalized as the problem of finding the controller $C(z) = \tilde{C}(z)U_1^T$ that minimizes the following cost-function:

$$J = \mathcal{E}\left(\varepsilon_k^T \varepsilon_k\right) + \rho\, \mathcal{E}\left(u_k^T u_k\right), \tag{4}$$

where $\rho \in \mathbb{R}, \rho > 0$ is a regularization parameter, which makes a trade off between the expected mean square residual phase error $\mathcal{E}(\varepsilon_k^T \varepsilon_k)$ and the expected amount of control effort $\mathcal{E}(u_k^T u_k)$. By increasing ρ it is possible to reduce the amount of energy dissipated by the DM and make to controller more robust to model uncertainties. In the limit that ρ goes to zero, minimizing cost-function (4) is equivalent to the classical criterion of minimizing the expected means square residual phase.

3. OPTIMAL CONTROL FOR AO

In this section we present a general recipe for determining the optimal controller that minimizes cost-function (4). It will be shown that the AO control problem can be conveniently expressed as an $\mathcal{H}_2$-optimal control problem. This implies that standard $\mathcal{H}_2$-optimal control theory can be used to compute the optimal controller. After summarizing the general solution to the $\mathcal{H}_2$-optimal control problem, we will briefly consider the specific case of a quasi-static AO system were the WFS and DM are assumed to be static and the only dynamics in the system is a unit-sample delay between measurement and correction. It will be shown that under the simplifying assumption of quasi-static operation it is possible to derive an analytical expression for the optimal closed-loop controller. Apart from being attractive from a computational point of view, the analytical solution is useful as it provides some additional insight in the relation with the common AO control approach.

3.1. The $\mathcal{H}_2$-optimal control framework

In this subsection we will briefly consider the standard $\mathcal{H}_2$-optimal control problem and its solution. The starting point of the $\mathcal{H}_2$-optimal control framework is the definition of the so-called generalized plant. Figure 2 provides a schematic representation of a such generalized plant. The generalized plant framework makes a clear distinction

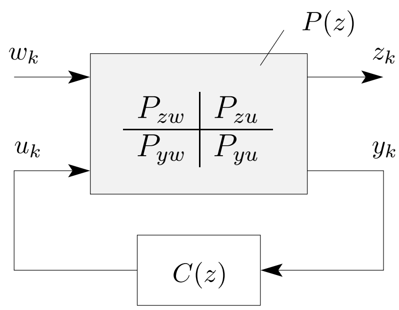

Figure 2. Block-diagram of closed-loop generalized plant representation

between exogenous zero-mean white noise inputs w_k and controller inputs u_k on the one hand and measurement outputs y_k and performance outputs z_k on the other hand. As common in most $\mathcal{H}_2$-optimal control literature, the zero-mean white noise input is assumed to have unit covariance, i.e. $\mathcal{E}(w_k^T w_k) = I$. Like the atmospheric disturbance model S, the generalized plant P will be represented in state-space form. For notational convenience the state update equation and the output equations will be combined to arrive at the following compact matrix description:

$$\left[\begin{array}{c} \xi_{k+1} \\ \hline z_k \\ y_k \end{array}\right] = \left[\begin{array}{c|cc} \mathcal{A} & \mathcal{B}_v & \mathcal{B}_u \\ \hline \mathcal{C}_z & \mathcal{D}_{zw} & \mathcal{D}_{zu} \\ \mathcal{C}_y & \mathcal{D}_{yw} & 0 \end{array}\right] \left[\begin{array}{c} \xi_k \\ \hline w_k \\ u_k \end{array}\right], \tag{5}$$

where the state of the generalized plant is denoted by ξ_k. To facilitate the discussion, it is useful to partition the generalized plant P in the same way as the input and output signals. As already indicated in Figure 2, the input-output relation is described in terms of four open-loop transfer functions, which will be denoted as $P_{zw}(z), P_{zu}(z), P_{yw}(z)$ and $P_{yu}(z)$. The subscripts in this notation refer to the corresponding partitioning of the input and output signals.

Given a generalized plant P, $\mathcal{H}_2$-optimal controller synthesis deals with the problem of finding the causal controller $C(z)$ that minimizes the influence of the zero-mean white noise input w_k on the performance output z_k. The influence of the white noise input on z_k is quantified by the $\mathcal{H}_2$-norm of the closed-loop transfer function from w_k to z_k. Let the closed-loop transfer function from w_k to z_k be denoted as $P_{zw}^{cl}(z) \triangleq P_{zw} + P_{zu}C(I - P_{yu}C)^{-1}P_{yw}$, then the $\mathcal{H}_2$-norm of $P_{zw}^{cl}(z)$ is defined as:

$$\|P_{zw}^{\mathrm{cl}}(z)\|_{\mathcal{H}_2}^2 \triangleq \sqrt{\frac{1}{2\pi}\mathrm{Tr}\int_{-\pi}^{\pi} P_{zw}^{\mathrm{cl}}(\mathrm{e}^{j\omega})P_{zw}^{\mathrm{cl}}(\mathrm{e}^{j\omega})^*\mathrm{d}\omega},$$

where $\cdot^*$ denotes the complex conjugate transpose and Tr is the trace operator. Using the above definitions, the $\mathcal{H}_2$-optimal control problem can be formalized as:

$$C(z) = \arg\min_{C(z)} \|P_{zw}^{\mathrm{cl}}(z)\|_{\mathcal{H}_2}^2. \tag{6}$$

The following Lemma provides a solution to the $\mathcal{H}_2$-optimal control problem. The $\mathcal{H}_2$-optimal controller is given in state-space form.

Lemma 3.1 (State-space solution to discrete-time $\mathcal{H}_2$-optimization problem[5,6]). *Consider the generalized plant $\mathcal{P}$ with state-space representation* (5)*, and assume that*

1. *the pair $(\mathcal{A}, \mathcal{B}_u)$ is stabilizable and the pair $(\mathcal{A}, \mathcal{C}_y)$ is detectable;*

2. $\mathcal{D}_{zu}^T\mathcal{D}_{zu} > 0$ *and* $\mathcal{D}_{yw}\mathcal{D}_{yw}^T > 0$*;*

3. *the matrices*
$$\begin{bmatrix}\mathcal{A}-\lambda I & \mathcal{B}_u\\ \mathcal{C}_z & \mathcal{D}_{zu}\end{bmatrix}, \begin{bmatrix}\mathcal{A}-\lambda I & \mathcal{B}_v\\ \mathcal{C}_y & \mathcal{D}_{yw}\end{bmatrix}$$
have full rank for all $\lambda \in \mathbb{C}$ *such that* $|\lambda| = 1$.

Under these conditions, there exist unique $X = X^T \geq 0$ *and* $Y = Y^T \geq 0$ *such that the following pair of Riccati equations are satisfied*

$$\begin{aligned} X &= \mathcal{A}X\mathcal{A}^T - (\mathcal{A}X\mathcal{C}_y^T + \mathcal{B}_v\mathcal{D}_{yw}^T)(\mathcal{C}_yX\mathcal{C}_y^T + \mathcal{D}_{yw}\mathcal{D}_{yw}^T)^{-1}(\cdot)^T + \mathcal{B}_v\mathcal{B}_v^T &(7)\\ Y &= \mathcal{A}^TY\mathcal{A} - (\mathcal{A}^TY\mathcal{B}_u + \mathcal{C}_z^T\mathcal{D}_{zu})(\mathcal{B}_u^TY\mathcal{B}_u + \mathcal{D}_{zu}^T\mathcal{D}_{zu})^{-1}(\cdot)^T + \mathcal{C}_z^T\mathcal{C}_z. &(8)\end{aligned}$$

With $X = X^T \geq 0$ *and* $Y = Y^T \geq 0$ *the solution to equations* (7)-(8)*, define the matrices*

$$\begin{aligned} F &\triangleq (\mathcal{B}_u^TY\mathcal{B}_u + \mathcal{D}_{zu}^T\mathcal{D}_{zu})^{-1}(\mathcal{B}_u^TY\mathcal{A} + \mathcal{D}_{yw}^T\mathcal{C}_z) &(9)\\ F_0 &\triangleq (\mathcal{B}_u^TY\mathcal{B}_u + \mathcal{D}_{zu}^T\mathcal{D}_{zu})^{-1}(\mathcal{B}_u^TY\mathcal{B}_v + \mathcal{D}_{zu}^TD_{zw}) &(10)\\ L &\triangleq (\mathcal{A}X\mathcal{C}_y^T + \mathcal{B}_v\mathcal{D}_{yw}^T)(\mathcal{C}_yX\mathcal{C}_y^T + \mathcal{D}_{yw}\mathcal{D}_{yw}^T)^{-1} &(11)\\ L_0 &\triangleq (FXC_y^T + F_0\mathcal{D}_{yw}^T)(\mathcal{C}_yX\mathcal{C}_y^T + \mathcal{D}_{yw}\mathcal{D}_{yw}^T)^{-1}. &(12)\end{aligned}$$

Then, the optimal controller $C(z)$ *in state space form, which minimizes the* $\mathcal{H}_2$*-optimal control problem* (6)*, is given by*

$$\left[\begin{array}{c}\hat{\xi}_{(k+1|k)}\\ \hline u_k\end{array}\right] = \left[\begin{array}{c|c}\mathcal{A}+\mathcal{B}_uL_0\mathcal{C}_y - \mathcal{B}_uF - L\mathcal{C}_y & \mathcal{B}_uL_0 - L\\ \hline F - L_0\mathcal{C}_y & -L_0\end{array}\right]\left[\begin{array}{c}\hat{\xi}_{(k|k-1)}\\ \hline y_k\end{array}\right] \tag{13}$$

where $\hat{\xi}_{(k|k-1)}$ *represents the estimate of* ξ_k *given the measurements* y_i*,* $i \leq k-1$.

3.2. The AO problem in the $\mathcal{H}_2$-optimal controller framework

An important aspect in the AO control problem is that there is a difference between the closed-loop WFS signal y_k that is measured and the observable part of the residual wavefront ε_k that we try to minimize. The $\mathcal{H}_2$-optimal control framework provides an attractive way to deal with this discrepancy between measurement and control objective. The AO system considered in this paper can be easily extended to fit in the generalized plant framework. By moving the system boundaries and considering the atmospheric disturbance model as a part of the AO system, it is possible to replace the exogenous input ψ_k by the zero-mean white noise signal v_k. As the zero-mean white noise signal v_k has a covariance matrix R_v different from identity, the system obtained by joining the atmospheric disturbance model and the standard AO system still doesn't fit in the generalized plant framework. For $R_v > 0$, this problem can easily be solved by defining a new system input w_k which is related to v_k as $v_k = R_v^{1/2}w_k$. The generalized plant provides a complete description of the interaction between AO system components and the atmospheric disturbance model.

In order to express the original AO control problem in the $\mathcal{H}_2$ framework, it is still necessary to choose an appropriate performance output z_k. The performance output z_k should be chosen in such way that it is consistent with the AO control objective. This can be achieved by choosing the performance output as $z_k = [\,\varepsilon_k^T\ \sqrt{\rho}u_k^T\,]^T$. For this particular choice, the squared 2-norm of the performance output $\|z_k\|_2^2 = z_k^Tz_k$ becomes equal to the outcome of the cost-function (4) and the AO control problem reduces to the problem of finding the controller $C(z)$ that minimizes the mean square performance output z_k. The block-diagram in Figure 2 provides a schematic representation of the obtained generalized plant, with white noise input v_k, control input u_k, measurement output y_k and performance outputs ε_k and $\sqrt{\rho}u_k$.

To obtain a better insight in the structure of the generalized plant P depicted in Figure 2, it may be useful to consider the relation between the input and output signals. The relation between the inputs and outputs may be derived from the models and definitions introduced in Section 2. By substituting the relations $\varepsilon_k = \psi_k - \psi_k^{dm}$

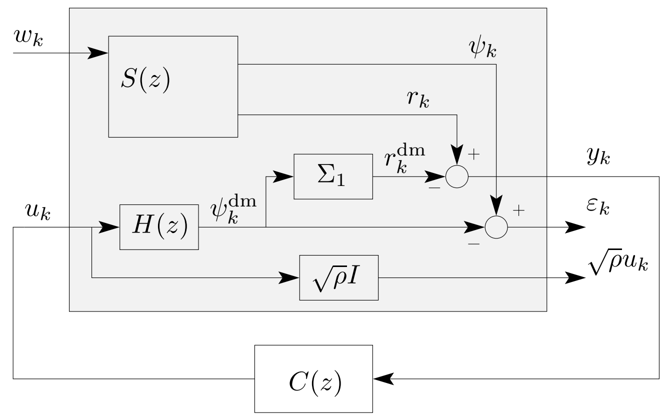

Figure 3. Block-diagram of a closed-loop AO system in generalized plant representation

and $\psi_k^{dm} = H(z)u_k$ in the reduced WFS senor model (1) and by applying the definition of r_k, we obtain the following expressions for the observable part of the residual phase ε_k and the corresponding WFS signal y_k:

$$\begin{array}{rcl} y_k & = & r_k - \Sigma_1 H(z) u_k \\ \varepsilon_k & = & \psi_k - H(z) u_k \end{array} . \tag{14}$$

With the open-loop WFS signal r_k and the observable part of the uncorrected wavefront distortion profile ψ_k being described by the atmospheric disturbance model (3), these equations fully explain the structure of the block-scheme in Figure 2. Furthermore, given the state-space realizations of the DM model $H(z)$, the WFS model $G(z)$ and the atmospheric disturbance model $S(z)$, the relations in equation (14) enable us to derive a state-space realization (5) of the generalized plant.

By introducing the generalized plant we have transformed to AO control problem to the problem of finding the controller that minimizes the mean square performance output z_k of a system of which the only exogenous input w_k is a zero-mean white noise signal. Since w_k is a white noise process with covariance matrix I, the mean square value of the performance output z_k can also be written in terms of the $\mathcal{H}_2$-norm of the closed-loop transfer function $P_{zw}^{\mathrm{cl}}(z)$. By using Parseval's theorem the mean square error of the signal z_k can be expressed as $\mathcal{E}\left(z_k^T z_k\right) = \|P_{zw}^{\mathrm{cl}}(z)\|_{\mathcal{H}_2}^2$. From this it is clear, that the AO control problem is equivalent to the standard $\mathcal{H}_2$-optimal feedback problem (6). In other words, a general strategy for computing the optimal AO controller for a given DM, WFS and atmospheric disturbance model, is to determine the generalized plant P via equation (1) and applying Lemma 3.1.

It may seem that the alternative formulation of the AO control problem does not account for the presence of measurement noise on the WFS slope measurement data, however the opposite is true. As already pointed out in Section 2, the contribution due to measurement noise is included in the description of open-loop WFS signal r_k by the atmospheric disturbance model. Just as in the problem of identifying the atmospheric disturbance model from open-loop WFS data, the controller is not able to make a distinction between the contribution due to the observable part of the residual wavefront distortion and the measurement noise. From a theoretical point of view it does make no difference whether the measurement noise is included in the atmospheric disturbance model or is modeled separately.

3.3. The $\mathcal{H}_2$-optimal AO controller in the quasi-static case

In the previous subsections we considered a general strategy to approach the AO control problem. In this subsection we will focus on what we call a quasi-static AO system. With a quasi-static AO system we refer to an AO system in which the DM and WFS can be considered to be static with a unit-sample delay in the loop of Figure 3. Under these conditions and the specific model structure for the atmospheric disturbance model (3), it is possible to derive an analytical expression for the optimal closed-loop controller. Having an analytical solution is attractive from a computational point of view as it avoids the need to solve the Riccati equations in Lemma 3.1. It also provides more insight in the relation with the common AO control approach, than the numerical solution. As the classical approach neglects all dynamics, i.e. the dynamics of the DM, WFS and atmosphere, the quasi-static case can be considered as a first order extension to the common AO control approach in which the atmosphere dynamics are included. In contrast to the common AO control approach, the quasi-static controller exploits the spatio-temporal correlation in the wavefront.

The assumption that the DM and WFS are static, implies that they can be described by a static matrix multiplication. Neglecting the dynamic behavior of the DM is quite realistic because in most astronomical AO systems the characteristic time of the DM is short compared to the sampling period.[7] On the other hand, the WFS usually acts as a broadband low-pass filter. Since the atmospheric disturbance has little contribution in the high frequency region, the dynamics introduced by the WFS can be neglected. Even though we neglect the dynamic behavior of the DM and WFS, it is important to consider the unavoidable one-sample delay between the moment of measuring a wavefront distortion and applying the correction. Incorporating this delay is also necessary to avoid an algebraic loop. Without loss of generality it is possible that the one sample delay introduced by the AO correction link is included in the DM model. Incorporating the delay in the DM model reduces the DM and WFS transfer functions $H(z)$ and $\tilde{G}(z)$ to:

$$H(z) = Hz^{-1} \quad \text{and} \quad \tilde{G}(z) = G \quad (\text{i.e. } \bar{G}(z) = I), \tag{15}$$

Starting from the above models for the WFS and DM it is possible to derive an explicit state-space representation of the generalized plant P. By substituting the quasi-static DM mirror model in equation (14) and using the state-space representation of the atmospheric disturbance model S to eliminate the signals r_k and ψ, we obtain the following expression for the generalized plant:

$$\begin{bmatrix} \xi_{k+1} \\ \hline \varepsilon_k \\ \sqrt{\rho} u_k \\ \hdashline y_k \end{bmatrix} = \left[\begin{array}{cc|c:c} 0 & 0 & 0 & I \\ 0 & A & KR_v^{1/2} & 0 \\ \hline -H & C & R_e^{1/2} & 0 \\ 0 & 0 & 0 & \sqrt{\rho} I \\ \hdashline -\Sigma_1 H & \Sigma_1 C & R_v^{1/2} & 0 \end{array}\right] \begin{bmatrix} \xi_k \\ \hline v_k \\ \hdashline u_k \end{bmatrix}, \tag{16}$$

where the state vector ξ_k is obtained by stacking a delay version of the input u_{k-1} and the state x_k of the atmospheric disturbance model, i.e. $\xi_k = \begin{bmatrix} u_{k-1}^T & x_k^T \end{bmatrix}^T$. To derive an analytical solution for the closed-loop optimal AO controller in the quasi-static case, Lemma 3.1 will be applied to the above generalized plant (16). Before applying the lemma, we will first proof that the necessary conditions are fulfilled. Stability of the atmospheric disturbance model (3) implies that the first condition of Lemma 3.1, on the stabilizability and detectability of the pairs $(\mathcal{A}, \mathcal{B}_u)$ and $(\mathcal{A}, \mathcal{C}_y)$, is satisfied. Furthermore, it can be easily checked that if $\rho > 0$ and $R^{1/2} > 0$, also the second condition is fulfilled. Since the matrix $R^{1/2}$ is the square root of a covariance matrix, failure of the condition $R^{1/2} > 0$ can only be due to a linear dependence between the channels of the zero-mean white noise disturbance signal v_k. When the atmospheric turbulence model is obtained by black-box identification from open-loop WFS data,[3] contaminated with measurement noise, this is very unlikely. In the unlikely event that nevertheless the condition $R^{1/2} > 0$ is not satisfied, it is always possible to find a projection that removes the linear dependence between the signals v_k which results in a disturbance model of reduced order. The condition of ρ being larger than zero is required to ensure that the term $\mathcal{D}_{zu}^T \mathcal{D}_{zu}$ is positive definite. Even though the regularization parameter ρ has to be chosen larger than zero in order to satisfy the second condition of Lemma 3.1, this condition can be potentially relaxed for the quasi-static case. When the matrix H has full column rank, the contribution of the control effort in cost-function (4) can be neglected by considering the limit in which ρ is going to zero. The third condition in Lemma 3.1 is equivalent to the requirement that the transfer functions $P_{zu}(z)$ and $P_{yv}(z)$ do not have zeros on the unit circle $\{z \in \mathbb{C} | \, |z| = 1\}$. From Figure 3 and the state-space realization of the atmospheric disturbance model S, it is clear that the transfer functions $P_{zu}(z)$ and $P_{yv}(z)$ can be expressed as:

$$P_{zu}(z) = \begin{bmatrix} -z^{-1} H \\ \sqrt{\rho} I \end{bmatrix}, \qquad P_{yv}(z) = R_v^{1/2} + \Sigma_1 C (zI - A)^{-1} K R_v^{1/2}. \tag{17}$$

From these equations it is clear that for $\rho \neq 0$ and $R^{1/2} > 0$ both transfer functions have no zeros on the unit circle. This implies that condition 3 of Lemma 3.1 is automatically satisfied whenever the second condition holds. With the generalized plant P satisfying all three conditions, the closed-loop optimal controller for the quasi-static case can be determined by applying Lemma 3.1. This results in the following main theorem:

THEOREM 3.2 (ANALYTICAL SOLUTION TO QUASI-STATIC AO CONTROL DESIGN PROBLEM). *Consider the quasi-static AO system with generalized plant* (16) *and assume that* $R_v^{1/2} > 0$. *When the matrix* H *has full column rank or* $\rho > 0$, *then the* $\mathcal{H}_2$*-optimal causal closed-loop controller* $C(z)$ *that is minimizing cost-function* (6) *has a state-space representation*

$$\left[\begin{array}{c} \hat{x}_{(k+1|k)} \\ \hline u_k \end{array}\right] = \left[\begin{array}{c|c} \widetilde{A} + K(\Sigma_1 H)H_\rho^\dagger C & K \\ \hline H_\rho^\dagger C\big(\widetilde{A} + K(\Sigma_1 H)H_\rho^\dagger C\big) & H_\rho^\dagger C K \end{array}\right] \left[\begin{array}{c} \hat{x}_{(k|k-1)} \\ \hline y_k \end{array}\right] \tag{18}$$

where the matrices $\widetilde{A}$, $\widetilde{C}$ *and* $H_\rho^\dagger$ *are defined as* $\widetilde{A} \triangleq A - K\Sigma_1 C$, $\widetilde{C} \triangleq \Sigma_1 C$ *and* $H_\rho^\dagger \triangleq (H^T H + \rho I)^{-1} H^T$, *respectively. Furthermore,* $\hat{x}_{(k|k-1)}$ *provides an optimal estimate of the state* x_k *of the atmospheric disturbance model* (3) *on the basis of the past closed-loop WFS measurements* $y_i, i < k-1$.

Proof. The proof of the theorem is included in Appendix A □

3.4. Relation with common AO control approach

The common AO control approach consists of a cascade of a static matrix multiplication and a series of parallel single-input single-output (SISO) feedback loops, which act as a temporal controller. Given a new WFS measurement, the static part is concerned with the problem of finding the deformable mirror (DM) actuator input that would provide the best fit to the wavefront, while parallel feedback loops are responsible for stability and closed-loop performance. The problem of determining the required static matrix multiplication is usually solved by considering maximum likelihood or maximum a posteriori techniques, under the simplifying assumption of open-loop operation. It is important to note that the WFS measures the residual and not the open-loop wavefront. The signal obtained after the static Reconstruction provides only an estimate of the correction that has to be applied to the actuator commands. To deal with this shortcoming the parallel feedback loops have to posses integrating action. In this paper we compare the performance of the $\mathcal{H}_2$-optimal controller with the following common AO control law:

$$u_k = \underbrace{(\tilde{H}^T\tilde{H})^{-1}\tilde{H}^T}_{F}\underbrace{(\tilde{G}^T\tilde{G} + \sigma_n^2 C_\phi^{-1}))^{-1}\tilde{G}^T}_{E}\frac{\beta}{1-\alpha z^{-1}}s_k, \tag{19}$$

where σ_n^2 is the variance of the measurement noise, C_ϕ is the spatial covariance matrix of the uncorrected wavefront and α and β are control parameters, which are usually determined on the basis of heuristic tuning rules. The matrices $\tilde{H}$ and $\tilde{G}$ are the static counterparts of the DM and WFS model $\tilde{H}(z)$ and $\tilde{G}(z)$ in the unreduced control problem of Figure 1. According to the separation principle the static matrix multiplication falls apart in a fitting operator F and estimation operator E. The operator E estimates the wavefront from the WFS measurements, while F provides a mapping of the estimated phase to the actuator inputs.

The $\mathcal{H}_2$-optimal controller in Theorem 3.2 has the special property that its state $\hat{x}_{(k|k-1)}$ provides an estimate of the state of the atmospheric disturbance model (3). This can be used to arrive at a nice physical interpretation. To this end, note that state-update and output equation differ only in the pre-multiplicative factor $H_\rho^\dagger C$. The output signal generated by optimal controller can therefore be expressed as $u_k = H_\rho^\dagger C\hat{x}_{(k+1|k)}$. Since $\hat{x}_{(k+1|k)}$ provides an estimate of the state of the atmospheric disturbance model, it follows from equation (3) that $C\hat{x}_{(k+1|k)}$ can be interpreted as an estimate of the observable part of the open-loop wavefront distortion ψ_{k+1}. By optimality of the state estimate $\hat{x}_{(k+1|k)}$, $\hat{\psi}_{(k+1|k)} \triangleq C\hat{x}_{(k+1|k)}$ is the optimal estimate of ψ_{k+1} on the basis of the past closed-loop WFS measurements $y_i, i \leq k$. On the other hand we recall that the matrix $H_\rho^\dagger$ can be seen as a regularized version of the pseudo-inverse of H and has the same function as the fitting operator F in the common control law (19). From this it is clear that the $\mathcal{H}_2$-optimal controller consists, just as the common control approach, of a succession of two operations, i.e. a one-step-ahead predictor which is concerned with the estimation of the observable part of the uncorrected wavefront ψ_k and a linear operator $H_\rho^\dagger$ which has the same function as the fitting operator F in equation (19). An important advantage with respect to the common control approach however, is that the $\mathcal{H}_2$-optimal controller is able to take full advantage of the spatio-temporal correlation in the wavefront and considers the wavefront estimation problem in a closed-loop setting. Furthermore, interpreting the closed-loop optimal controller as the cascade of a one-step-ahead predictor and a linear fitting problem demonstrates the close relation with predictive control.

4. VALIDATION STUDY

4.1. Closed-loop simulations on breadboard data

The proposed $\mathcal{H}_2$-optimal control approach has been validated for the quasi-static case on the basis of open-loop WFS data obtained from an AO test bench. The breadboard setup has a turbulence simulator that consists of a circular plan parallel glass plate rotated by a driving stage. On one side of the glass plate, distortions are etched such that the resulting wavefront has a spatial Kolmogorov spectrum with a $D/r_0 = 5$, where D is the diameter of the telescope and r_0 denotes the Fried parameter. This results in a single frozen layer disturbance. The setup uses a Shack-Hartmann WFS and an electrostatic DM with 37 actuators provided by OKO technologies. The simulations are performed on the basis of $N = 10^4$ samples obtained with a sampling frequency of $f = 25$Hz. The rotational speed of the glass plate results in a Greenwood frequency of $f_G = 0.95$Hz. Since the temporal error scales as $\sigma_T \sim (f_G/f)^{5/3}$, the temporal error remains the same if the sample frequency and Greenwood frequency are multiplied by the same factor. An AO system with for example a sample frequency of $f = 296$Hz has therefore an equivalent Greenwood frequency of $f_G = 11.25$Hz.

In the simulation experiments, the performance of quasi-static $\mathcal{H}_2$-optimal controller is compared with the common control law (19). The control parameter β has been tuned to optimize the closed-loop performance, which resulted in $\beta = 0.997$. The covariance matrix C_ϕ has been computed for a Kolmogorov spatial spectrum where the r_0 corresponds to the disturbance pattern etched on the glass plate. The variance of the measurement noise σ_n^2 has been estimated by recording the WFS measurements without the glass plate in place. Two scenarios will be elaborated. The first scenario comprises a closed-loop simulation with an ideal DM. An ideal DM is a mirror of which the influence matrix H can be inverted such that it can fully compensate the observable part of the wavefront. In the second scenario the influence matrix has been obtained experimentally from the DM in the AO setup. In all experiments the atmospheric disturbance model of order $n = 256$, is obtained from open-loop WFS measurements by using the identification method presented in the companion paper,[3] where the block-Hankel size is $q = 20$. The control effort weighting in cost-function (4) is neglected by choosing $\rho = 0$. To focus on the temporal dynamics of the controller, the performance is evaluated by considering the normalized averaged power spectrum P_ω of the observable part of the residual phase error. The power spectrum is normalized on the time averaged mean square value of the uncorrected wavefront ψ_k, which leads to the following definition:

$$P_\omega = N \frac{\sum_{j=1}^{m_r} \Phi_\omega^\varepsilon(j)}{\sum_{j=1}^{m_r} \sum_{k=1}^{N} \psi_k^2(j)}, \tag{20}$$

where $\Phi_\omega^\varepsilon(j)$ is the power spectrum of the j-th component of the observable part of the residual wavefront denoted as $\varepsilon_k(j) = \psi_k(j) - \psi_k^{dm}(j)$ evaluated at the frequency ω. To have a quantitative measure of the total reduction in mean square residual phase the following performance criterion is introduced:

$$J_1 = \frac{\sum_{j=1}^{m_r} \sum_{k=1}^{N} (\psi_k(j) - \psi_k^{dm}(j))^2}{\sum_{j=1}^{m_r} \sum_{k=1}^{N} \psi_k^2(j)}. \tag{21}$$

Also the simulation experiments are performed on the basis of open-loop WFS data. Figures 4 and 5 show the normalized averaged power spectra P_ω of the residual wavefront obtained in closed-loop simulations with the ideal and true DM. For the ideal mirror, the averaged residual power spectrum obtained with the optimal controller is approximately white. This means that, at least on average, there is no temporal correlation in the residue that can be used to further improve the performance of the controller. The residue obtained with the common AO control law on the other hand has a strong coloring. The normalized reductions obtained for the ideal DM are $J_1 = 0.0041$ for the common control approach and $J_1 = 0.0012$ for the optimal control approach. This is a reduction of 71%. The corresponding values obtained with the true DM are $J_1 = 0.0225$ and $J_1 = 0.0194$, which results in a reduction of 14%. The simulations show that the true DM severely limits the performance. Although there is still a reasonable reduction, these values are smaller than expected from the simulations performed in the companion paper. This is mainly caused by a 5 times lower wind-speed. This implies that the temporal error in the current simulations is approximately $5^{5/3} \approx 15$ smaller.

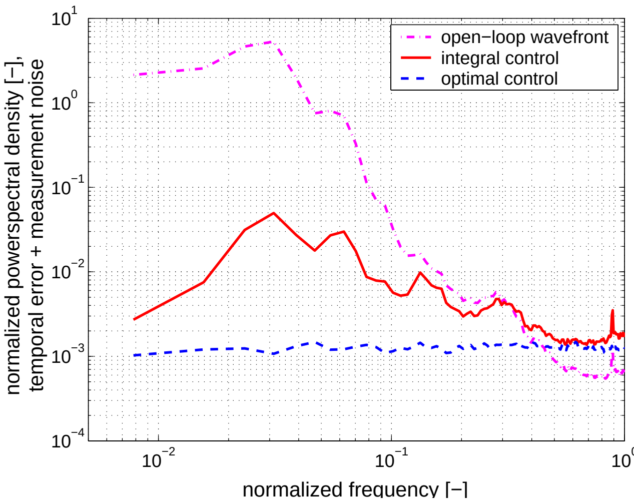

Figure 4. (Ideal DM) Normalized averaged power spectrum P_ω of the observable part of the residual wavefront ϵ_k for closed-loop simulations with an ideal DM.

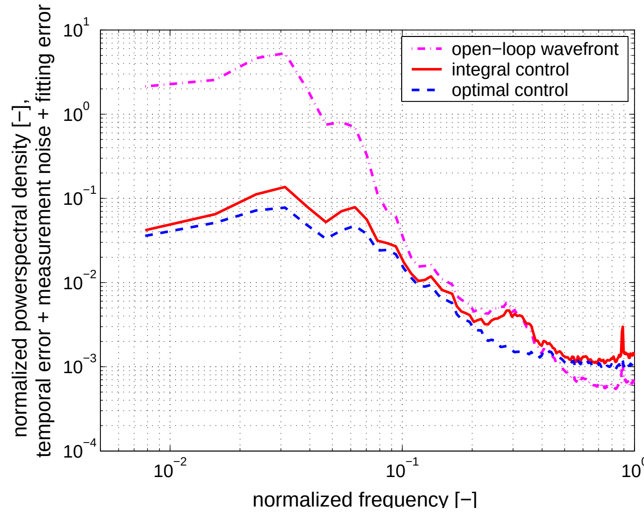

Figure 5. (Breadboard DM) Normalized averaged power spectrum P_ω of the observable part of the residual wavefront ϵ_k for closed-loop simulations with the breadboard DM.

4.2. Sensitivity study of closed-loop performance to WFS measurement noise

In this subsection we investigate the influence of measurement noise on the performance of the closed-loop controller. The objective is to find out if the $\mathcal{H}_2$-controller can be used to reduce the signal to noise ratio (SNR) requirement to achieve a specified performance J_1, which enables the use of a fainter guide star. The first step in the simulation procedure is to estimate the SNR of the unreduced open-loop WFS signal s_k obtained from the breadboard. The SNR obtained from 1500 samples undistorted WFS measurements is 27dB. The observed measurement noise is due to a combination of photon noise, CCD readout noise, background noise and residual turbulence in the lab. To generate open-loop WFS signals with different SNRs, zero-mean white noise[1,8] is added to each of the channels of the WFS measurements s_k, i.e.: $\tilde{s}_k = s_k + \eta_k^r + \eta_k^a$, where $\tilde{s}_k$ is the generated noise contaminated WFS signal, η_k^r the noise on the measured data and η_k^a is artificially added white noise. The variance of the noise sequence $\eta_k^a(j)$ added to the j-th component of the WFS signal $s_k(j)$ is such that the this channel has a specified SNR given by:

$$SNR(j) = 10 \log_{10} \left(\frac{\sum_{k=1}^{N} s_k^2(j)}{\sum_{k=1}^{N} (\eta_k^r(j) + \eta_k^a(j))^2} \right).$$

The presented $\mathcal{H}_2$-optimal control approach tries to minimize the observable part of the reconstructed residual wavefront ϵ_k, which includes the effect of measurement noise. As long as the noise is white, the presented approach will be optimal because white noise cannot be predicted. When the measurement noise is colored however, the measurement noise will interfere with the estimate of the reconstructed wavefront which results in a discrepancy between the desired and actual control objective. This can only be avoided by using separate models of the atmospheric disturbance and the contribution due to the WFS measurement noise. Because it is not possible to make a distinction between measurement noise and the contribution due to the residual wavefront distortion, these models can not be obtained from measurement data only.

In the simulation we use a different noise realization of the identification of the disturbance model and the evaluation of the closed-loop performance. For each SNR, the experiment is repeated 5 times of which the averaged reduction in mean square residual phase J_1 is depicted in Figures 6 and 7. Figure 6 corresponds to the performance simulated with the ideal DM ,while Figure 7 shows the performance for the true DM. Since the SNR is expressed in dBs, both axes in the figures are on a logarithmic scale. The figures show that for low SNRs there is an exponential relation between the reduction J_1 and the SNR. In the simulations, the cost-function J_1 is normalized on the mean square uncorrected phase ψ_k without being contaminated by measurement noise. For high SNR the reduction in mean square error deviates from this trend. In the simulations with the ideal DM this deviation is explained by the contribution of the real measurement noise on the open-loop WFS signal s_k. Since the SNR of the open-loop WFS measurement signal is in the order of 27dB, it is not possible to generate input signals with SNRs better that 27dB. A least squares fit of the logarithm of the normalized cost-function J_1 to the SNRs in the range from -5 to 15 dB in Figure 6, gives rise to the following exponential relations:

$$J_1 = 0.367 \cdot 10^{-0.0872\,\mathrm{SNR}} \text{ (common)}, \qquad J_1 = 0.281 \cdot 10^{-0.0939\,\mathrm{SNR}} \text{ (optimal)} \tag{22}$$

The above relation is depicted by the solid and dashed lines in Figures 6 and Figure 7. From this it is clear that for low SNRs, the performance in the simulations with the true DM follow the same exponential trend. In the simulations with no-ideal DM, the fitting error becomes the limiting factor for signal to noise ratios higher that approximately 17dB. The gain in performance obtained by optimal controller decreases for decreasing values of the SNR. This is understandable since the measurement noise contains no information for prediction. In analyzing the performance, it is important to note that the comparison is not entirely fair as the common controller (19) uses prior information on the signal to noise ratio. The variance of the open loop noise σ_n^2 is used in the common controller (19). In the presented simulations the variance of the measurement noise is precisely known. In practice this parameter has to be estimated from the data. The $\mathcal{H}_2$-optimal control approach described in this paper doesn't need this information.

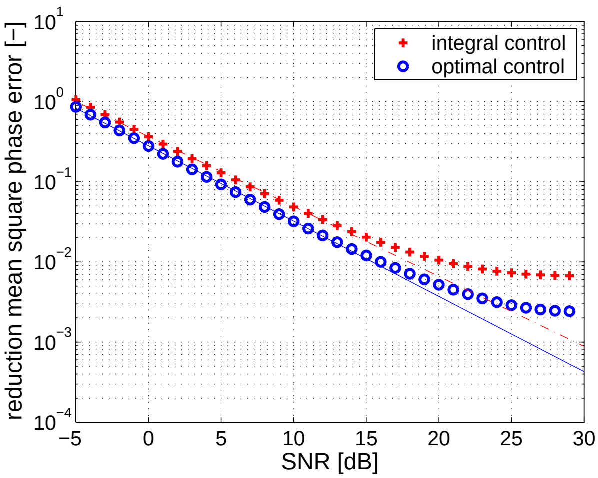

Figure 6. (Ideal DM) Averaged mean square residual phase error J_1 as a function of the SNR. The mean square phase error is normalized on the mean square value of the (noise-free) uncorrected wavefront ϕ_k.

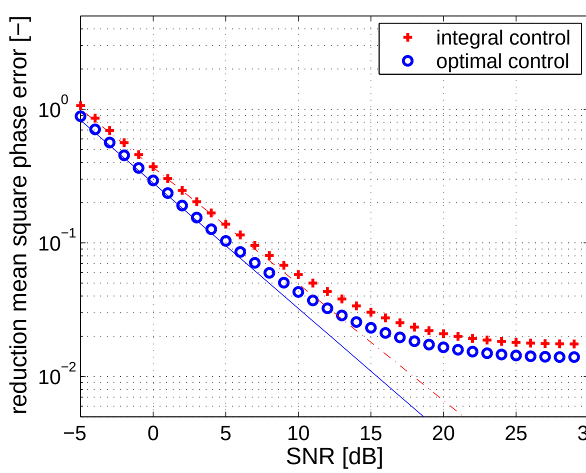

Figure 7. (Breadboard DM) Averaged mean square residual phase error as a function of the SNR. The mean square phase error is normalized on the mean square value of the (noise-free) uncorrected wavefront ϕ_k.

Under the assumption that the WFS is photon noise limited, the fitted exponential relation (22) between SNRs and the reduction in mean square residual phase, can be exploited to relate a specified performance level J_1 to the difference in upper-bound on the magnitude of the guide stars required for both controllers. For a photon limited WFS the SNR (in this case expressed as a ratio of mean square errors and not in dBs) of the measurement signal s_k is proportional to the n_{ph}, where n_{ph} is the number of photons per sub-aperture[1,2] per sensor integration time. By using the definition of the magnitude scale the ratio of photons required by both controllers for specified performance level J_1 can be expressed as a magnitude difference:

$$\Delta m = -2.5 \log_{10} \left(\frac{n_{ph}^{opt}}{n_{ph}^{int}} \right) = 0.22 - 0.21 \log_{10}(J_1), \tag{23}$$

where n^{opt} is the number of photons per sub-aperture per sensor integration time required by the optimal control approach and n^{int} the equivalent for the common approach. The relation shows that the limiting magnitude, i.e. magnitude from which AO is effective in reducing the wavefront distortion ($J_1 < 1$), differs 0.22 for both methods. When the required reduction is 0.01 the magnitude difference is becomes 0.66.The corresponding lower bounds on the required SNRs are 17.9dB for the integral controller and 15.4dB for the optimal controller.

5. CONCLUSIONS

In this paper we have formulated the AO control problem in a $\mathcal{H}_2$-optimal control framework. Given a linear time invariant (LTI) description of the deformable mirror (DM) $H(z)$, the wavefront sensor (WFS) $G(z)$ and an atmospheric disturbance model $S(z)$, in which the uncorrected wavefront and the open-loop wavefront signal are described as filtered white noise, $\mathcal{H}_2$-optimal control theory provides a standard tool to compute the closed-loop optimal control. By using an appropriate disturbance model it is possible to account for the spatio-temporal correlation in the wavefront. The specific case of a quasi-static AO system, where the WFS and DM are assumed to be static and only dynamics in the system is a unit-sample delay between measurement and correction, has been elaborated in detail. The closed-loop optimal controller is expressed in terms of an analytical solution, which provides a nice physical interpretation. It shows that the closed-loop optimal controller can be interpreted as an one-step ahead predictor of the uncorrected wavefront distortion followed by a static projection of the estimated wavefront on the actuator space.

The solution for a quasi-static AO system has been demonstrated by means of numerical validation experiments on open-loop WFS data. In these experiments the performance is compared with the common AO control approach. The validation experiments show that the optimal control results in a performance improvement. For an ideal DM, the mean square residual phase error has been reduced by more than 71%. By including the true DM in the simulations the gain in performance reduces to 14%. In this case the DM fitting error is clearly the limiting factor. This demonstrates the relevance of solid budgeting of error contribution of the different components of the AO system. If the temporal error and measurement noise limit the performance, optimal control is able to reduce the overall error significantly.

The influence of measurement noise on the closed-loop performance has been investigated. The sensitivity study shows that it is possible to trade the gain in performance achieved by $\mathcal{H}_2$-optimal controller against a reduction in signal to noise ratio (SNR) which enables the use of a fainter guide star. The experimentally determined relation between performance and SNR, has been used to relate a specified performance level to the difference in guide star magnitude needed by the optimal control and common control approach. Even though the relation only holds for the considered simulation conditions it shows that the gain in magnitude increases with the required performance level. In the simulations, the gain in performance is modest with the gain expected from the simulations in the companion paper.[3] This is caused by the relative small temporal error, which in this paper is approximately 15 times smaller due to the lower wind-speed. This underlines *once again* the importance of investigating the conditions under which optimal control is most effective.

ACKNOWLEDGMENTS

This research has been conducted in the framework of the "Knowledge Center for Aperture Synthesis". The knowledge center is an initiative of TNO Science and Industry to develop fundamental and advanced technologies for optical aperture synthesis. The knowledge center is a long-term co-operation of TNO and primarily the Delft University of Technology.

REFERENCES

1. J. Hardy, *Adaptive Optics for Astronomical Telescopes*, Oxford University Press, New York, 1998.
2. F. Roddier, *Adaptive Optics in Astronomy*, Cambridge University Press, 1999.
3. K. Hinnen, M. Verhaegen, and N. Doelman, "$\mathcal{H}_2$-optimal control of an adaptive optics system, part I: Data-driven modeling of the wavefront phase disturbance," in *Astronomical Adaptive Optics Systems and Applications II*, *Proc. of SPIE* **5903**, pp. 1–8, (Bellingham), Aug. 2005.
4. M. Born and E. Wolf, *Principles of Optics: Electromagnetic Theory of Propagation*, Cambridge University Press, seventh (expanded) edition ed., 1999.
5. H. Shu and T. Chen, "State-space approach to discrete-time $\mathcal{H}_2$ optimal control with a causality constraint," in *Proceedings of the 34th Conference on Decision and Control*, pp. 1927–1932, (New Orleans, LA), Dec. 1995.
6. T. Chen and B. Francis, *Optimal Sampled-Data Control Systems*, Springer-Verslag, London, Berlin, 1995.
7. B. L. Roux, J.-M. Conan, C. Kulcsár, H.-F. Raynaud, L. Mugnier, and T. Fusco, "Optimal control law for classical and multiconjugate adaptive optics," *Journal of the Optical Society of America. A* **21**, pp. 1261–1276, jul 2004.
8. E. Gendron and P. Lena, "Astronomical adaptive optics," *Astronomy and Astrophysics* **291**, pp. 337–347, 1994.
9. *Introduction to mathematical system theory: a behavioral approach*, Texts in applied mathematics, Springer-Verslag, New York, 1998.

APPENDIX: PROOF OF THEOREM

Consider the discrete-time algebraic Riccati equation (7). By substituting the state-space realization of the generalized plant (16) and partitioning the matrix X in accordance with the partitioning of the state-transfer matrix $\mathcal{A}$, the Riccati equation can be expressed as

$$\begin{bmatrix} X_{11} & X_{12} \\ X_{21} & X_{22} \end{bmatrix} = \begin{bmatrix} 0 & 0 \\ 0 & AX_{22}A^T + KR_vK^T + VZ^{-1}V^T \end{bmatrix},$$

where V and Z are functions of X defined as $V(X) \triangleq -AX_{21}(\Sigma_1 H)^T + AX_{22}(\Sigma_1 C)^T + KR_v$ and $Z(X) \triangleq \mathcal{C}_y X \mathcal{C}_y^T + R_v$. From the above equation it is clear that the matrices X_{11}, X_{12} and X_{22} are all zero. When these matrices are substituted in the functions $V(X)$ and $Z(X)$, the above equation reduces to a lower dimensional Riccati equation in the unknown X_{22}. The solution to the Riccati equation (7) is therefore given by:

$$X = \begin{bmatrix} X_{11} & X_{12} \\ X_{21} & X_{22} \end{bmatrix} = \begin{bmatrix} 0 & 0 \\ 0 & \bar{X} \end{bmatrix}$$

where $\bar{X} \triangleq X_{22}$ satisfies the reduced Riccati equation

$$\bar{X} = A\bar{X}A^T + \left[A\bar{X}(\Sigma_1 C)^T + KR_v\right]\left((\Sigma_1 C)\bar{X}(\Sigma_1 C)^T + R_v\right)^{-1}\left[\,\cdot\,\right]^T + KR_vK^T \tag{24}$$

and $[\,\cdot\,]^T$ is used as a shorthand to denote the transpose of the first term between square brackets. Let us now consider the second Riccati equation (8). Following the same approach of substituting the generalized plant P and partitioning the matrix Y, the Riccati equation can be written as

$$Y = \begin{bmatrix} Y_{11} & Y_{12} \\ Y_{21} & Y_{22} \end{bmatrix} = \begin{bmatrix} H^T H & -H^T C \\ -C^T H & * \end{bmatrix} \tag{25}$$

where the asterisk denotes a sub-matrix that depends on the unknown Y but does not influence the matrices F, F_0, L and L_0. Equation (25) specifies therefore the relevant part of the matrix Y. Substituting the obtained relations for X and Y into definition (9) to (12), yields the following expressions for F, F_0, L and L_0

$$F = -\begin{bmatrix} 0 & H_\rho^\dagger C A \end{bmatrix} \qquad F_0 = -H_\rho^\dagger C K R_v^{1/2}$$

$$L = \begin{bmatrix} 0 \\ K \end{bmatrix} \qquad L_0 = -H_\rho^\dagger C \bar{K}$$

where $\bar{K} \triangleq \left(A\bar{X}(\Sigma_1 C)^T + KR_v\right)\left((\Sigma_1 C)\bar{X}(\Sigma_1 C)^T + R_v\right)^{-1}$ and $H_\rho^\dagger$ is defined as in Theorem 3.2. It is important to note that the matrix $\bar{K}$ is precisely the Kalman gain corresponding to the Riccati equation (24). Since the atmospheric disturbance model provides a minimum phase representation of the open-loop WFS measurement signal r_k, this implies that $\bar{K} = K$. The derived expressions for F, F_0, L and L_0 give rise to the following state-space realization of the closed-loop optimal controller $C(z)$

$$\left[\begin{array}{c} u_k \\ \hat{x}_{(k+1|k)} \\ \hline u_k \end{array}\right] = \left[\begin{array}{cc|c} H_\rho^\dagger CK(\Sigma_1 H) & H_\rho^\dagger C(A - K(\Sigma_1 C)) & -H_\rho^\dagger CK \\ K(\Sigma_1 H) & A - K(\Sigma_1 C) & -K \\ \hline -H_\rho^\dagger CK(\Sigma_1 H) & -H_\rho^\dagger C(A - K(\Sigma_1 C)) & H_\rho^\dagger CK \end{array}\right] \left[\begin{array}{c} u_{k-1} \\ \hat{x}_{(k|k-1)} \\ \hline y_k \end{array}\right]. \qquad (26)$$

The above state-space realization is of order $n_u + n$, but the order of the optimal controller can be reduced by considering the Kalman decomposition,[9] which disentangles the system in a controllable and an autonomous part. The following similarity transformation of the state provides such a decomposition

$$\begin{bmatrix} u_{k-1} \\ x_k \end{bmatrix} (= \xi_k) \longrightarrow T^{-1} \begin{bmatrix} u_{k-1} \\ x_k \end{bmatrix}, \quad \text{where} \quad T = \begin{bmatrix} -I & H_\rho^\dagger C \\ 0 & -I \end{bmatrix}.$$

Since the uncontrollable part of the state-space representation has no influence on the input-output behavior of the controller, it can be removed without changing the overall control performance. In this way we obtain the state-space realization of the $\mathcal{H}_2$-optimal controller as given in Theorem 3.2. Another result of Lemma 3.1 is that the state in the state-space equations (26) provide an optimal estimate of the state $\xi_k = [\, u_{k-1}^T \; x_k^T \,]^T$ of the generalized plant. By applying the similarity transformation $\xi_k \rightarrow T^{-1}\xi_k$ and removing the autonomous part of the state, it is clear that the state $x_{(k|k-1)}$ of the controller $C(z)$ in Theorem 3.2 state provides an estimate of the state of the atmospheric disturbance model (3), given the closed-loop measurements $y_i, i < k-1$.